

Article

Shaking Table Testing of a Low-Rise Reinforced Concrete Intermediate Moment Resisting Frame

Sida Hussain ¹, Hamna Shakeel ¹, Asif Ali ¹, Muhammad Rizwan ²  and Naveed Ahmad ^{3,*} ¹ Department of Civil Engineering, UET Peshawar, Peshawar 25000, Khyber Pakhtunkhwa, Pakistan² Department of Civil Engineering, SUIT Peshawar, Peshawar 25000, Khyber Pakhtunkhwa, Pakistan³ Department of Civil and Environmental Engineering, Stanford University, Stanford, CA 94305, USA

* Correspondence: dmaveed@stanford.edu

Abstract: Multi-level shaking table tests were performed on a 1:3 reduced scale two-story reinforced concrete (RC) intermediate moment resisting frame (IMRF) conforming to the requirements given in the ACI-318-19. The exterior joints lacked shear reinforcement to assess the viability of the ACI model recommended for determining the design shear strength of the beam–column joint panel. One of the horizontal components of the 1994 Northridge earthquake accelerogram (090 CDMG Station 24278, Source: PEER strong motion database) was input to the frame for multi-level shaking table testing. Plastic hinges developed in beams under base input motion with a maximum acceleration equal to 0.40 g. The exterior joints incurred extensive damage under base input motion with a maximum acceleration equal to 0.70 g. The frame achieved displacement ductility and overstrength factors (determined as the ratio of the maximum resistance of the frame to the design base shear force) equal to 2.40 and 2.50, respectively. This gives a response modification factor equal to 6. The satisfactory performance of the frame is attributed to the high efficiency of the beam–column joint, which was confined by spandrel beams on two faces and the high strength of the concrete. The inherent minimal confinement is sufficient to ensure satisfactory seismic behavior. The analysis confirmed overstrength equal to 1.58 for joint shear strength in comparison to the design strength determined using the ACI model. The data might serve as a reference for calibrating and validating numerical modeling techniques for performance evaluation, which are crucial in the context of performance-based engineering.

Keywords: joint shear capacity; overstrength; ductility factor; IMRF; reinforced concrete



Citation: Hussain, S.; Shakeel, H.; Ali, A.; Rizwan, M.; Ahmad, N. Shaking Table Testing of a Low-Rise Reinforced Concrete Intermediate Moment Resisting Frame. *Buildings* **2022**, *12*, 2104. <https://doi.org/10.3390/buildings12122104>

Academic Editors: Rafael Shehu, Nicola Tarque and Manuel Buitrago

Received: 21 October 2022

Accepted: 29 November 2022

Published: 1 December 2022

Publisher's Note: MDPI stays neutral with regard to jurisdictional claims in published maps and institutional affiliations.



Copyright: © 2022 by the authors. Licensee MDPI, Basel, Switzerland. This article is an open access article distributed under the terms and conditions of the Creative Commons Attribution (CC BY) license (<https://creativecommons.org/licenses/by/4.0/>).

1. Introduction

A ductile frame exhibits reduced lateral stiffness and increased energy dissipation that tends to reduce seismic forces relative to forces that would occur in a linearly elastic frame [1–3]. Therefore, such a frame can be designed for the lower seismic force given in seismic code ASCE/SEI-7-22 [4]. It is achievable if frames are properly detailed to attain such ductile behaviour. Therefore, the IBC-2021 [5] relies primarily on the ACI-318-19 [6] code that lists design procedures and minimum requirements for ductile detailing. The structural frame members are intended to resist design basis earthquake motion through ductile response but without critical deterioration of strength.

The ASCE/SEI-7-22 permits the use of an intermediate moment-resisting frame (IMRF) as a lateral load-resisting system for frames assigned to the seismic design category (SDC) B and C. The code suggests it may also be permitted as part of dual systems for frames assigned to SDC D, E, and F. In the later, the IMRF is designed for a portion of a lateral load (e.g., 25% of total base shear) but intended to deform in congruence with the dual system. The SDC assigned to a frame depends on the intended use and occupancy of the building and the ground motions at the site. The IBC-2021 suggests the building should be assigned to the more severe SDC.

Based on the observations from past experimental tests performed on interior and exterior beam–column sub-assemblages [7], the ACI-318-19 recommends transverse reinforcement in beam–column joints unless the joint is restrained on all four sides by beams. The joint transverse reinforcement is intended to confine the joint concrete and preclude longitudinal column bar buckling. This requirement is relieved when the beam framing into the joint extends from the opposite face of the joint up to a length at least equal to the beam depth [8], ensuring the extending beam/column members are properly dimensioned and reinforced to provide effective restraints to the joint. This research discusses a field practice in which lateral ties are not provided in the joint panel due to installation challenges, which is common in most underdeveloped countries. This research proposes to improve the behavior of such frames by employing high-strength concrete and spandrel beams to confine joints, and to confirm this through dynamic shaking table tests. The ACI model that was used in the design is also examined for application to a similar problem for structural design and verification.

The present research confirms through a series of shake-table tests performed on a two-story IMRF that if the exterior beam–column joint is confined by appropriately detailed spandrel beams on two faces and the joint concrete has compressive strength equal to/greater than 28 MPa, the joint efficiency will improve. The frame achieved strength and toughness sufficient to resist design basis earthquake ground motions without deterioration of strength. One of the horizontal components of the 1994 Northridge earthquake accelerogram (090 CDMG Station 24278, Source: PEER strong motion database) was selected as input motion to the frame. The selected frame was tested progressively (using a single input motion linearly scaled to multiple hazard levels) until the joint capacity was fully exhausted and the frame was found to be in a near collapse state. The joint efficiency was quantified and compared with the joint shear strength obtained using the ACI model given in the ACI-318-19 to assess the efficacy of the design strength model for the considered frame.

The ACI-318-19 suggests the exterior beam–column joints of the intermediate moment-resisting frame should have transverse reinforcements that are distributed within the column height equal to the beam depth. This shear reinforcement is based on the requirements of ACI-352R [9] and intends to prevent deterioration due to shear cracking and buckling of longitudinal column reinforcement. The present research confirms through shake-table tests that such stringent requirements may be relaxed especially for low-rise intermediate moment-resisting frames when the exterior joints are confined by beams on three faces and concrete has compressive strength equal to or more than 28 MPa. The inherent minimal joint confinement is sufficient to ensure satisfactory seismic behavior.

2. Design of Selected Moment-Resisting Frame

2.1. Lateral Seismic Forces

The selected frame is a two-story one-bay moment-resisting frame (Figure 1). The preliminary member sizes chosen and material properties considered for the frame are reported in Table 1. The seismic base shear force V for the frame was computed in accordance with the equivalent lateral force procedure given in the ASCE/SEI-7-22:

$$V = C_S W. \quad (1)$$

Table 1. Preliminary chosen sizes of beams and columns and basic material properties.

Member	Depth in. (mm)	Width in. (mm)	Clear Span in. (mm)	f_c' ksi (MPa)	E_c ksi (GPa)	f_y ksi (MPa)	E_s ksi (GPa)
Beams:	18 (457)	12 (305)	204 (5182)	4 (28)	3605 (24.86)	60 (414)	29,000 (200)
Columns:	12 (305)	12 (305)	138 (3505)	4 (28)	3605 (24.86)	60 (414)	29,000 (200)

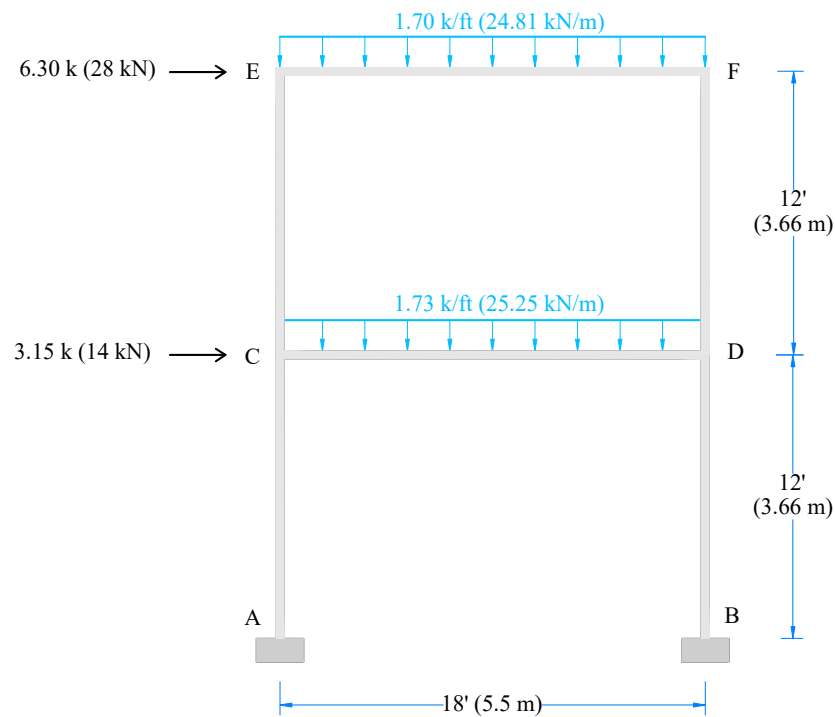


Figure 1. Selected moment-resisting reinforced concrete frame.

The value of seismic response coefficient C_S depends on a number of geotechnical parameters and seismicity of the site and the type of structural system used to resist lateral seismic forces. Table 2 reports the values considered for the selected frame. The value of C_S was determined in accordance with the procedure given in the ASCE/SEI-7-22 (12.8.1.1). The response modification coefficient R needs attention, as this accounts for reduction of the design spectral response acceleration for ductile frames capable of dissipating seismic energy through inelastic deformation in the hinging regions of members. The ASCE/SEI-7-22 recommends taking $R = 5.0$ for an intermediate moment-resisting frame. Moreover, the selected frame was assigned to SDC C and earthquake importance factor I_e was taken as equal to 1.25. The Rayleigh method and eigenvalue analysis of the elastic frame model provide accurate estimates of the fundamental vibration period of frames [10]; however, the fundamental vibration period of frame $T = 0.42$ s was computed in accordance with the empirical equation suggested in the ASCE/SEI-7-22 (12.8.2.1), which is based on the earlier work of Goel and Chopra [11,12], which provides a conservative estimate of the seismic response coefficient. The upper limit coefficient C_u was taken as 1.5 in accordance with the ASCE/SEI-7-22 for the selected design spectral response acceleration parameter. This results in a seismic response coefficient C_S equal to 0.118, which was increased by 30 percent (i.e., $C_S = 1.3 \times 0.118 \approx 0.15$) in accordance with the orthogonal seismic loads combination procedure proposed in the ASCE/SEI-7-22 (C12.5.3) based on the earlier work of Veletsos and Newmark [13]. The design base shear force V is equal to 42.42 kN. The lateral seismic forces $F_x = [28 \text{ kN}, 14 \text{ kN}]$ for roof and first floor, respectively, were computed in accordance with the vertical distribution factor C_{vx} given in ASCE/SEI (12.8.3).

Table 2. Geotechnical, seismic and structural parameters considered for the design of frame.

SDC	S_{DS}	S_{D1}	Soil	I_e	R	Ω_o	C_d
C	0.5	0.2	B	1.25	5.0	3	4.5

2.2. Design of Beams

The beams were designed for flexure and shear actions in accordance with ACI-318 (18.4.2). The design of the beams was based on the demands for beam member CD, since it

will be subjected to higher bending and shear actions. Figure 2 shows the factored design moment M_{ub} for combined gravity and lateral seismic forces. Positive bending moments are plotted below the beam centroid and negative moments are plotted above the centroid. The ACI-318-19 mention the beam should have at least two continuous longitudinal bars at both top and bottom faces. For this reason, and to simplify the construction of the test frame, three longitudinal steel bars of 19 mm were selected for both top/bottom faces of the beam. The nominal moment strength M_{nb} of the selected doubly reinforced beam section was calculated through an iterative procedure as described by Wight [14]. For the properties of the material given in Table 1, a value of $M_{nb} = 133$ kN·m and the reduced nominal moment strength ϕM_{nb} equal to 120 kN·m were determined. The demand-to-capacity ratio of the selected beam is 0.85 which gives a flexural overstrength equal to 1.17. This indicates the appropriateness of the selected tension reinforcement for the top face of the beam. Under lateral seismic load reversal, the reinforcement in the bottom face of the beam will develop similar flexural strength in tension.

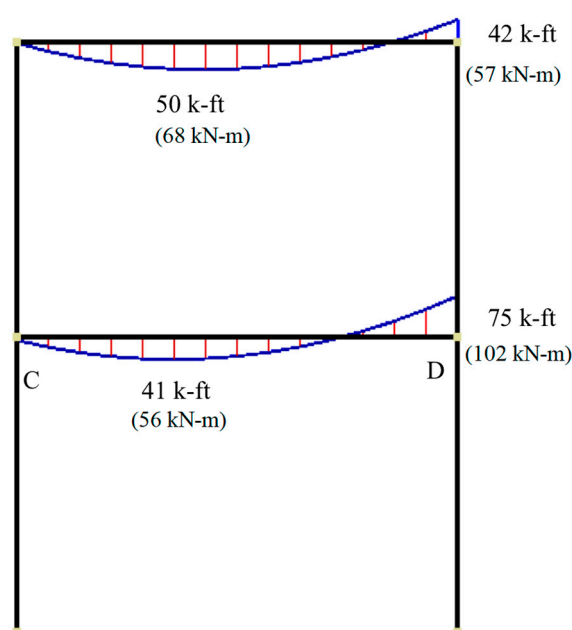


Figure 2. Factored design moment M_{ub} for beams for combined gravity and lateral seismic forces.

The factored shear force was computed in accordance with the ACI-318-19 (18.4.2.3) which suggests two procedures for determining shear: a) based on the free body diagram and assuming that nominal moment strengths (taking $\phi = 1$) are developed at both ends of the beam, and (b) analyzing the frame for lateral seismic forces including the earthquake effects doubled, i.e., $2E$. For the present case, procedure (a) gives value 7% higher than procedure (b). Figure 3 shows the considered factored design shear V_{ub} for combined gravity and lateral seismic forces.

The nominal shear strength V_{nb} was calculated in accordance with the ACI-318-19 (22.5.1) for one-way shear. In comparison with the classical model for the shear strength of concrete V_{cb} [15], the updated models now include the effects of member depth and the longitudinal reinforcement ratio on shear strength [16,17]. This is due to the fact that the beams with increased depth and reduced area of longitudinal reinforcement exhibit lower shear stress at failure [18–21]. The updated model gives a value equal to 48.26 kN for reduced nominal shear strength of concrete ϕV_{cb} . This is 31% less than the previous simple model [16]. The shear reinforcement was computed in accordance with the ACI-318-19 (22.5.8.5.3). In present case, 9.53 mm double-leg stirrups were used as shear reinforcement, taking the longitudinal spacing s of the shear reinforcement as equal to 76 mm. The demand-to-capacity ratio computed for shear reinforcement is 0.55. The section still maintains a demand-to-capacity ratio equal to 0.72, even if the concrete component is ignored. This

gives shear overstrength equal to 1.40. Moreover, the appropriateness of the selected cross-sectional dimensions was also checked in accordance with the ACI-318-19 (22.5.1.2), which gives a demand-to-capacity ratio of 0.42, indicating the efficacy of the selected sizes of beam cross-sections. The designed shear reinforcement also conforms to the provisions of the ACI-318-19 (18.4.2.4).

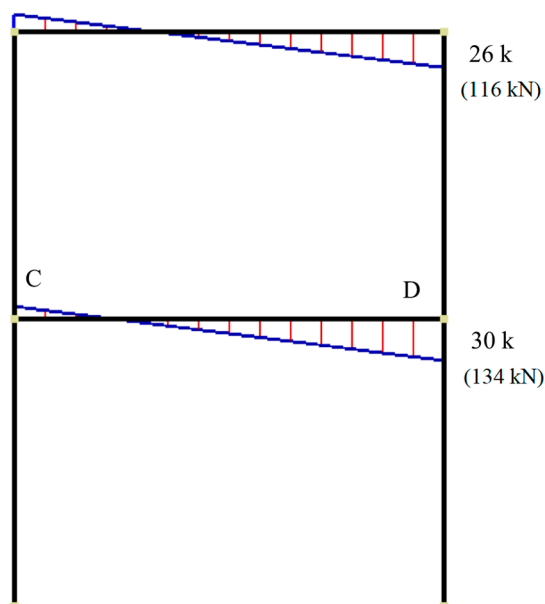


Figure 3. Factored design shear V_{ub} for beams in accordance with ASCE/SEI-7-16 (18.4.2.3).

2.3. Design of Columns

The beams of the frame are designed as yielding members while columns and beam–column joints are capacity-protected through appropriate dimensions and detailing. This is intended to ensure a strong-column and weak-beam lateral load-resisting frame for seismic energy dissipation without compromising the stability of the frame [22]. However, the additional requirement of the ACI-318-19 (18.7.3.2) that recommends flexural strengths of the special moment resisting columns should satisfy the criteria $\sum M_{nc} \geq (6/5) \sum M_{nb}$ is compromised for intermediate moment-resisting frames; the factor (6/5) is equal to 1. Therefore, factored moments M_{uc} for columns were computed for the combined gravity and lateral seismic forces (Figure 4). The design of the columns was based on the member BD, since ground story columns are subjected to higher combined actions (moment, axial, shear, and story-drift). The column design moments were further increased to take into account the flexural overstrength of the beam (i.e., 1.17). Values of 64 kN·m and 196 kN were obtained for design moment M_{uc} and the corresponding axial force P_{uc} , respectively.

The selected columns were assumed as having eight 19 mm longitudinal bars. Likewise, the nominal moment strength M_{nc} of the selected column section was calculated through an iterative procedure as described by Wight [14]. For the properties of the material given in Table 1, values of $M_{nc} = 81$ kN·m and the reduced nominal moment strength ϕM_{nc} equal to 73 kN·m were determined for the tension-controlled section with pre-compression P_{uc} . The demand-to-capacity ratio of the selected column is 0.87 which gives a flexural overstrength equal to 1.15. This indicates the appropriateness of the selected reinforcement for the column section.

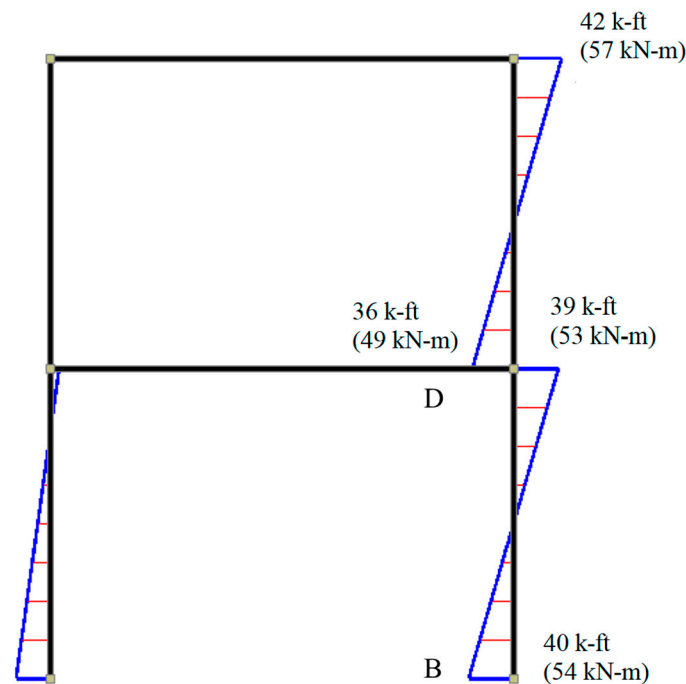


Figure 4. Factored design moment M_{uc} for columns for combined gravity and lateral seismic forces.

The factored shear force for the column was computed in accordance with the ACI-318-19 (18.4.3.1) which suggests procedures given in the ACI-318-19 (18.4.2.3) for beam shear. However, the earthquake effect E is increased by an overstrength factor Ω_o equal to 3.0. Figure 5 shows the factored design shear force for columns. Likewise, the nominal shear strength V_{nc} was calculated in accordance with the ACI-318-19 (22.5.1). Similarly, 9.53 mm double-leg stirrups were used as shear reinforcement of columns taking the longitudinal spacing s equal to 76 mm. The demand-to-capacity ratio computed for shear reinforcement is equal to 0.33, and it is equal to 0.40 if the concrete component is ignored. This gives shear overstrength equal to 2.50 and confirms the appropriateness of the selected shear reinforcement.

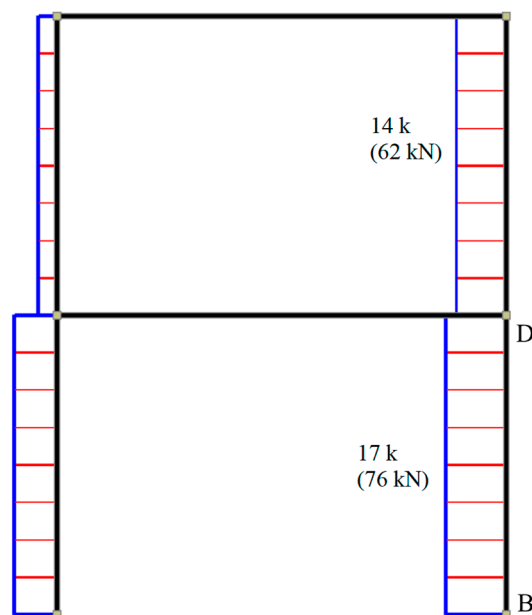


Figure 5. Factored design shear V_{uc} for columns for combined gravity and lateral seismic forces.

2.4. Design of Beam–column Joints

The beam–column joints of the test frame were confined on all three faces: a main beam resisting in-plane loads and two transverse beams of similar sizes and reinforcement. The design of joint C is discussed. The joint shear $V_{u,joint}$ was computed in accordance with the ACI-318-19 (18.4.4.7.1). This requires horizontal shear force on a plane at mid-height of the joint $V_{u,joint}$ to be calculated using Equations (2) and (3), as described by Wight [14]:

$$V_{u,joint} = T_{pr} - V_{col} \quad (2)$$

$$T_{pr} = \alpha A_S f_y. \quad (3)$$

Moreover, the ACI-318-19 suggests using tensile and compressive beam forces and column shear consistent with beam nominal moment strength M_{nb} . Therefore, parameter α is equal to 1.0. The tensile force T_{pr} is equal to 356 kN. For $M_{nb} = 9133$ kN-m, V_{col} is equal to 311 kN. The nominal joint shear strength $V_{n,joint}$ was computed in accordance with the ACI-318-19 (18.8.4.3) using Equation (4):

$$V_{n,joint} = 15\lambda\sqrt{f'_c}A_j. \quad (4)$$

The modification factor λ is equal to 1.0 for normal concrete. The joint area A_j is taken as equal to 92,903 mm². The value of $V_{n,joint}$ is found equal to 610 kN. This gives nominal joint shear strength $\phi V_{n,joint}$ equal to 366 kN. The demand-to-capacity ratio was found equal to 0.86, indicating joint shear overstrength equal to 1.17 for design base actions. This shows the efficacy of the considered joint laterally supported by beams on three faces and the high compressive strength of concrete. In the present research, the shake-table tests will also confirm the efficiency of the considered joint. Figure 6 shows the reinforcement details of the selected beam/column members and beam–column joint panels for test frames.

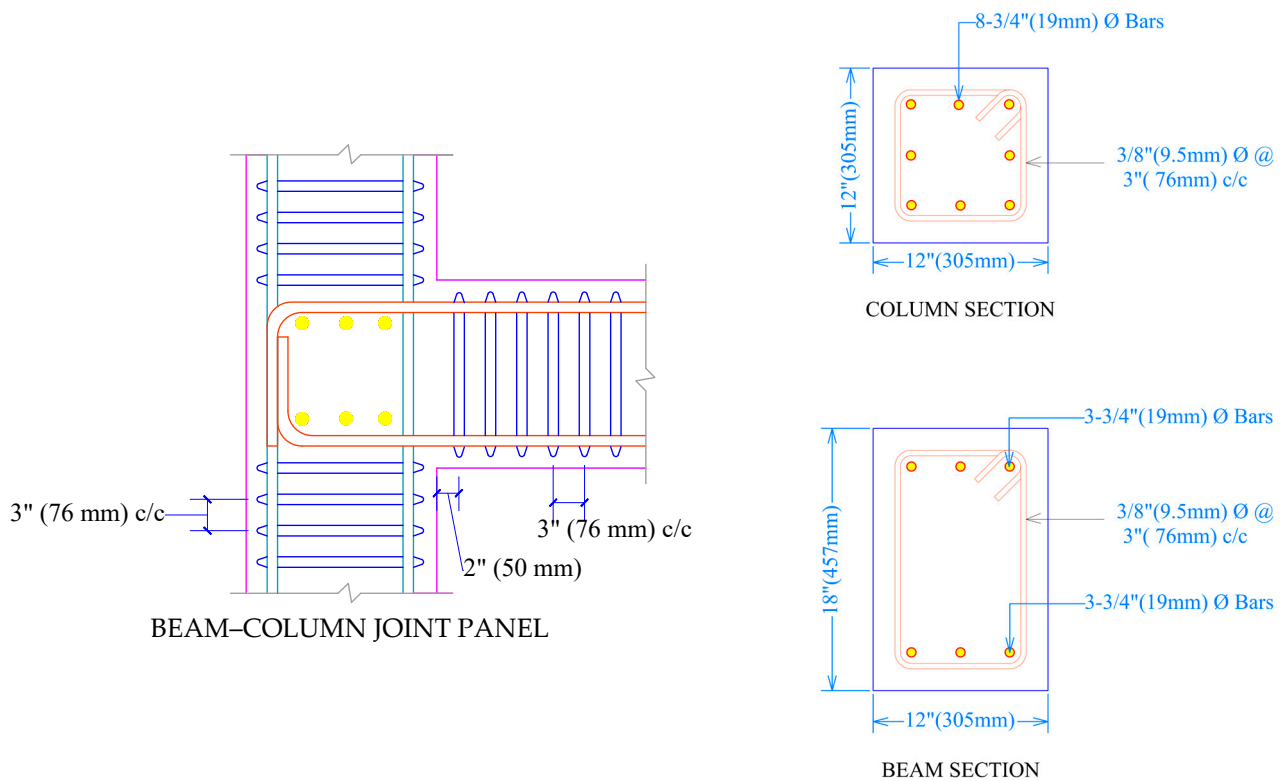


Figure 6. Geometric and reinforcement details of the beam/column members and panel.

3. Shake-Table Tests on Selected Frame

Figure 7 shows the 1:3 reduced-scale test frame prepared using the similitude requirements for a simple model. The linear dimensions of beam/column members, slab, and diameter of reinforcement were reduced by a scale factor $S_L = 3$. The concrete used constituents in a mix proportion as 1:1.68:1.72 (cement: sand: aggregate) with water-to-cement weight equal to 0.48, in order to achieve the required compressive strength of concrete. The test frame model was also provisioned with additional floor mass M_{mf} in accordance with the similitude requirements for dynamic seismic analysis of the model, as described in Moncarz and Krawinkler [23]:

$$M_r = \frac{M_p}{M_m} = S_L^2 \quad (5)$$

$$M_{mf} = \frac{M_{p1}}{S_L^2} - M_{m0}. \quad (6)$$

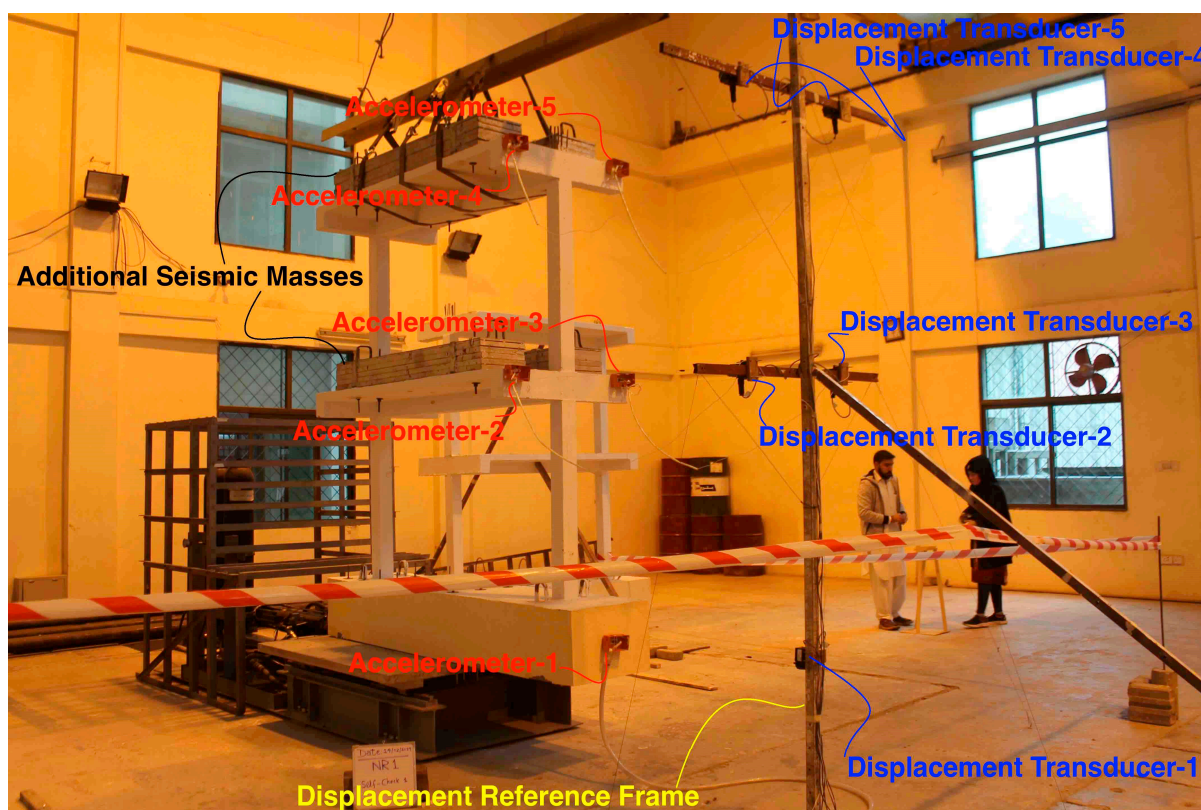


Figure 7. A 1:3 reduced scale test frame.

An additional floor mass equal to 5.90 kN was applied on each floor using steel blocks of 300 kg on each side of the main beam. The weights were placed outside the effective width of beam. Two displacement string pots and two accelerometers were mounted at the mid-height of the slab at each floor level on transverse beams, in order to measure response histories of floor displacements and floor accelerations. One string pot and accelerometer were also mounted at the base of the model to measure the actual input base motions.

The acceleration time history of 1994 Northridge Mw 6.7 earthquake was selected for input base motion. This was recorded at the Castaic Old Ridge RT, 090 CDMG Station 24278, having the closest distance of 22.60 km to fault rupture. Figure 8 shows the design response spectrum for parameters given in Table 2 and the scaled acceleration response spectrum of the selected accelerogram. The scaling is performed by linearly matching the spectral accelerations of accelerogram and the design spectrum at the fundamental time period of frame ($T = 0.42$ s). Moreover, the accelerogram was time-compressed by a factor

of $S_L^{1/2} = 3^{1/2}$ to satisfy the similitude requirement [24] for the base input motion of 1:3 reduced scale test frame.

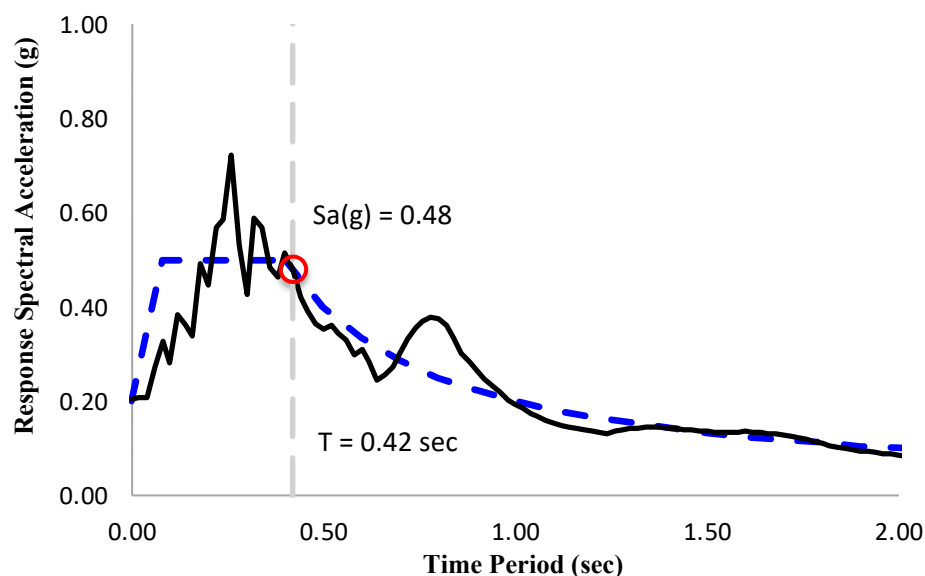


Figure 8. Scaled acceleration response spectrum of Northridge-1994 for base motions.

Table 3 reports the values of measured sustained maximum accelerations (the value of the acceleration which is reached or exceeded at least three times) at the base of models for a series of test runs. The observed damages in each test are also reported in Table 3 and shown in Figures 9–11. The test frame exhibited horizontal and vertical flexural cracks at the beam–joint interface, which were aggravated with the increasing amplitude of base motions. The beam–column joint panels incurred extensive damages under base motions with a sustained maximum acceleration equal to 0.70 g.

Table 3. Measured sustained maximum acceleration of base motions of the test frame.

Test Runs	PHA * (g)	Remarks
1	0.20	-
2	0.40	Horizontal and vertical flexural cracks at the beam–joint interface.
3	0.45	Aggravation of horizontal flexural cracks at the beam ends. Occurrence of slight cracks in beam–column joints
4	0.70	Extensive damages occurred at the beam–column joint panels on both floor levels.

* Peak horizontal acceleration.

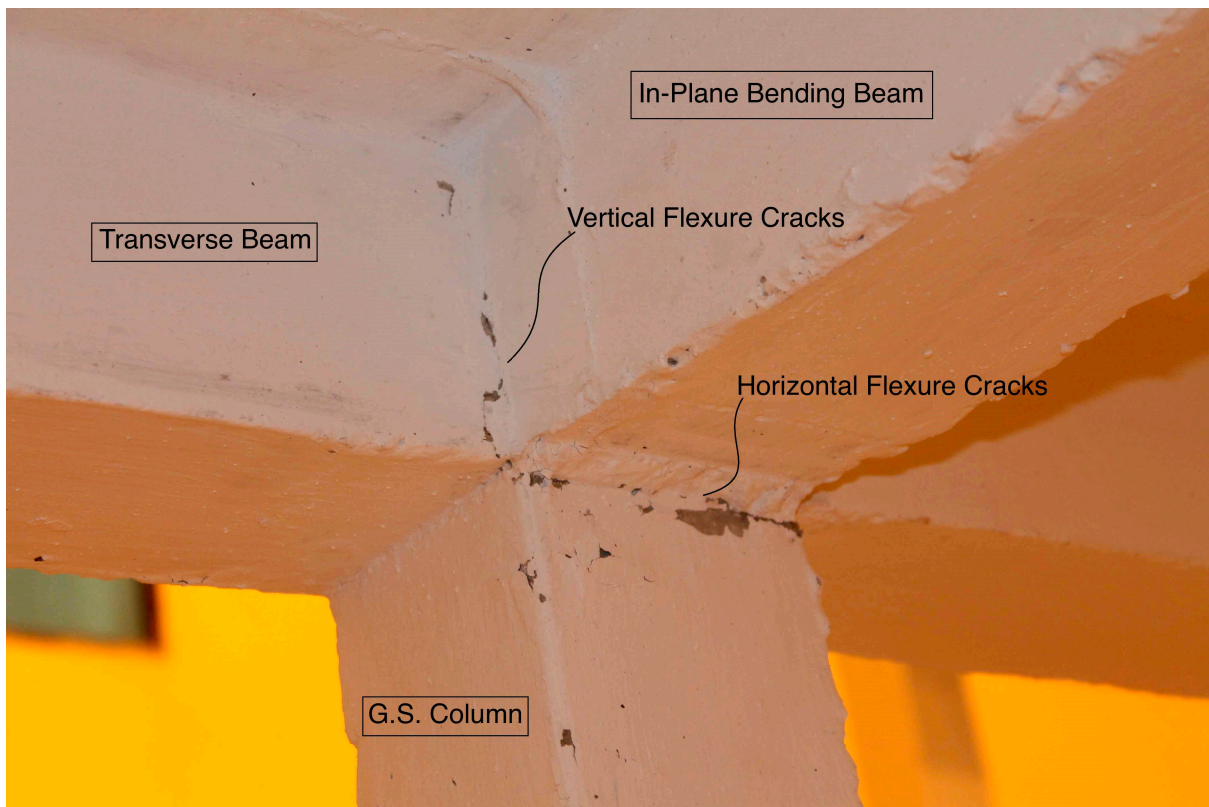


Figure 9. Horizontal and vertical flexural cracks at the beam–joint interface under test run 2 (ref. Table 3). G.S. column refers to the ground story column.

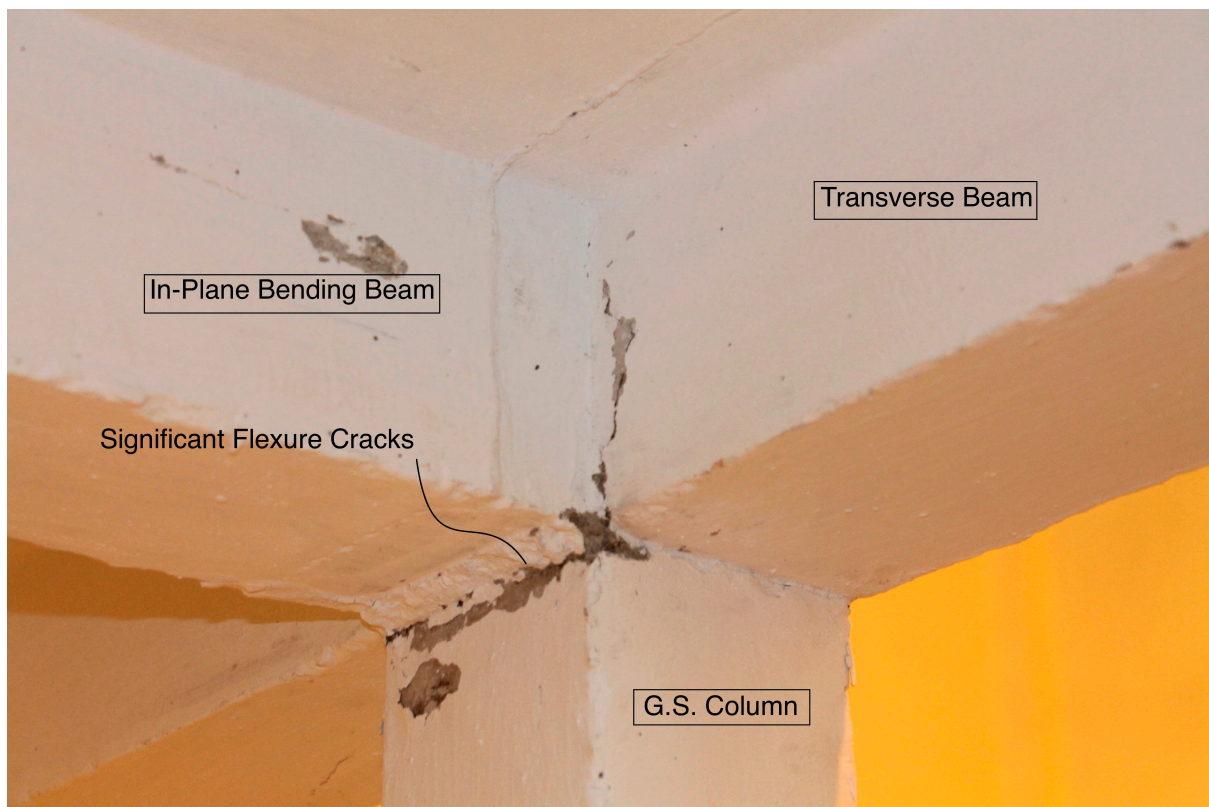


Figure 10. Aggravation of horizontal flexural cracks at the beam ends under test run 3 (ref. Table 3). G.S. column refers to the ground story column.



Figure 11. Extensive damage occurred at beam–column joint panel under test run 4 (ref. Table 3).

4. Seismic Design Factors for Selected Frame

4.1. Overstrength Factor

The beam/column members of the selected frame were designed with capacities greater than the design forces. It is most likely the actual material strength is higher than the nominal strength specified in the design. Moreover, the test frame also comprised the slab that acts monolithically with the beam. These sources are likely to increase the actual maximum lateral strength (V_{max}) of the frame in comparison to the design lateral strength (V). The ratio of the V_{max} to V is referred to as the overstrength factor Ω_o . The ASCE/SEI-7-22 suggests Ω_o equal to 3 for IMRF.

The measured response histories of floor accelerations and displacements for all test runs were processed to compute the relative displacement of the roof and the corresponding base shear force for the prototype of the test frame. The first three runs were analyzed to develop a force-displacement capacity curve for the prototype of the tested frame (Figure 12). The capacity curve exhibits a hardening response in the post-yield state. The ASCE/SEI 7-22(12.12) suggests the allowable story drift of $0.020 h_{sx}$ for the selected frame that was considered as the maximum drift for computing the peak base shear force. A value equal to 106 kN is obtained. This gives an overstrength factor equal to 2.50, which is 20% less than the value suggested by the ASCE/SEI-7-22 for the selected frame.

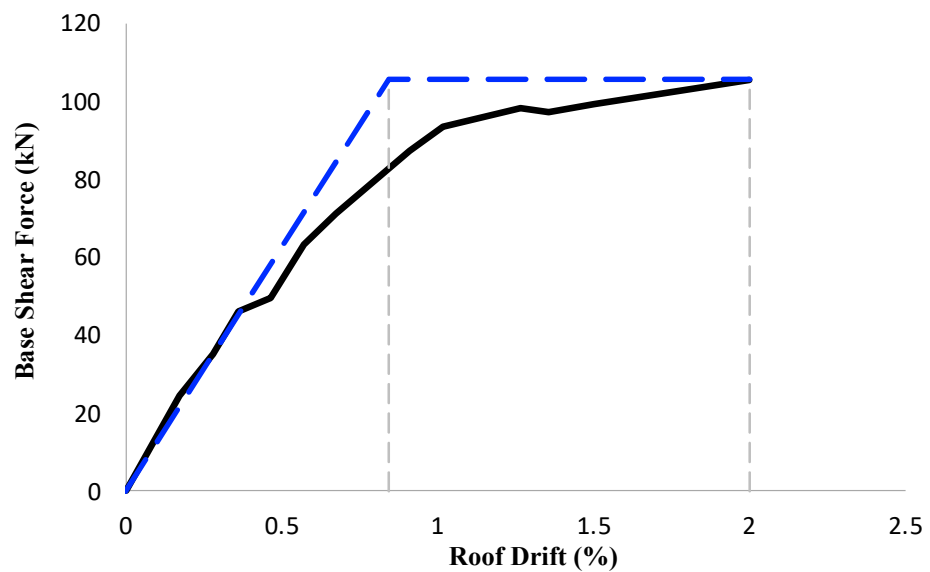


Figure 12. Force-displacement capacity curve for a prototype of tested frame.

Figure 13 shows the considered plastic mechanism of the selected frame for the analytical prediction of peak base shear force. The virtual work method was used to compute V_{max} using Equations (7) and (8):

$$W_{ve} = W_{vi} \quad (7)$$

$$0.835V_{max} = \theta(4M_{pb} + 2M_{pc}) \quad (8)$$

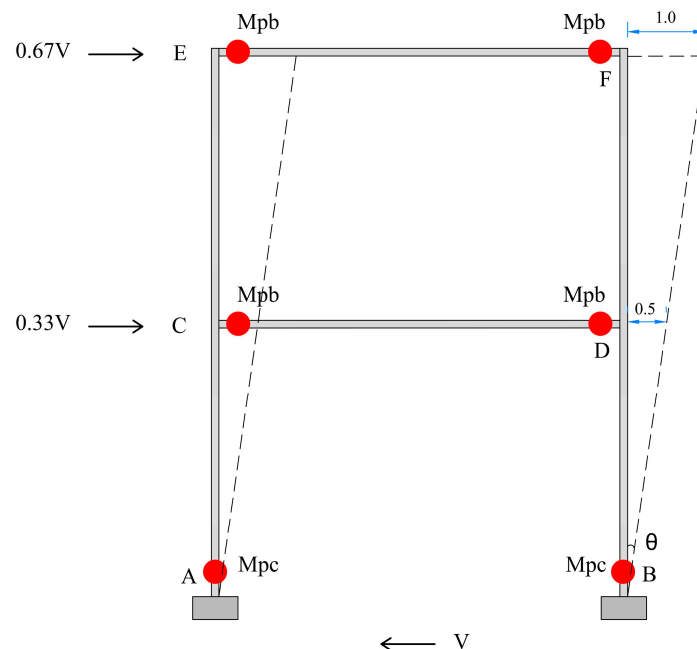


Figure 13. Considered plastic mechanism of the selected frame.

For $M_{pb} = 133 \text{ kN}\cdot\text{m}$, $M_{pc} = 81 \text{ kN}\cdot\text{m}$, $\theta = 1/24 \text{ rad}$ ($1/7.315 \text{ rad}$) and V_{max} equal to 113.62 kN is obtained. This gives an overstrength factor equal to 2.68, which is approximately 11% less than the value suggested by the ASCE/SEI-7-22 and 7.20% higher than the value obtained using the experimental force-displacement curve. This confirms the

efficacy of the simplified analytical method for computing the peak base shear force at the maximum permissible drift.

4.2. Ductility Factor

The ductility factor of a frame is a measure of its global nonlinear response, which is related to the global displacement ductility of the frame [25]. The global effective yield displacement Δ_y was obtained using the FEMA-P695 procedure [26]. Considering the allowable story drift of $0.020 h_{sx}$ as the maximum permissible drift, the displacement ductility ratio μ was found equal to 2.40 ($\mu = \Delta_{max}/\Delta_y \approx 2.40$). The bi-linearized capacity curve gives a yield vibration period T_y of frame equal to 0.72 s for the first mode of vibration assuming linear deflected shape, which is greater than 0.50 s. Thus, the ductility factor R_μ is taken as equal to the displacement ductility ratio, i.e., $R_\mu = \mu = 2.40$ in accordance with the suggestion of Newmark and Hall [25].

Alternatively, the effective yield displacement was computed in accordance with the suggestion of Priestley et al. [27] in order to assess the efficacy of the simplified analytical prediction. The yield drift of a story for the reinforced concrete frame is computed using Equation (9):

$$\theta_y = 0.5\varepsilon_y \frac{L_b}{h_b}. \quad (9)$$

For $\varepsilon_y = 0.0021$, $L_b = 5486$ mm and $h_b = 457$ mm, the yield drift is equal to 1.24. It is sufficiently accurate to approximate the global effective yield drift of the frame equal to story drift for a linear deflected frame shape under lateral seismic forces. This gives a displacement ductility ratio equal to 1.61, which is 33% less than the ductility ratio obtained based on the experimental global nonlinear response curve. This significant difference is due to the fact that the analytical model given in Equation (9) is based on the response of beam–column connection sub-assemblages that did not include the slab. Nevertheless, this analytical model is conservative for design purposes.

4.3. Response Modification Coefficient

This factor is used to calculate the seismic response coefficient required for the determination of seismic base shear using the equivalent lateral force procedure given in the ASCE 7-16 for seismic design of frame. For a frame, the response modification coefficient R is described as the product of the overstrength factor Ω_o and the ductility factor R_μ , i.e., $R = \Omega_o \times R_\mu$. The experimental data gives R equal to 6.0 ($R = 2.50 \times 2.40 = 6.0$), which is 20% higher than the value suggested in the ASCE 7-22 for the selected frame (i.e., $R = 5$). This increase is due to the higher ductility capacity of the tested frame.

The analytical predictions based on the virtual work method for computation of peak base shear and the empirical formula suggested by Priestley et al. for computation of effective yield displacement gives R equal to 4.31 ($R = 2.68 \times 1.61 = 4.31$), which is 28% less in comparison to the R factor obtained using the experimental data. The analytically computed R factor (i.e., 4.31) is approximately 14% less than the value suggested in the ASCE 7-22. This confirms that simplified analytical models give a conservative value for the response modification coefficient.

5. Assessment of Beam–Column Joint

5.1. Efficiency of Beam–Column Joint

The efficiency of a joint is the measure of its reserve strength. For a connection, this is computed as the ratio of the force causing the failure of the joint to the force corresponding to the moment capacity of the yielding beam entering the joint. For a global frame, the efficiency of the considered beam–column joint, which is laterally supported by beams on three faces, was determined by computing the ratio of the base shear force causing failure of the joint V_f to the base shear force (V_{max}) developed at the maximum permissible drift under design base earthquake (Figure 14). The efficiency of joint is equal to 1.56 or 156%. The measured efficiency is significantly higher than the values reported for typical

corner joints subjected to bending causing the opening of the joint [28,29]. This is due to the fact that the considered beam–column joint was laterally supported by beams on two faces in addition to the in-plane beam entering the joint. Moreover, the corresponding roof deflection capacity determined is equal to 4.70%, which is 135% higher than the maximum permissible drift under design base earthquake. Considering the maximum considered earthquake (MCE) ground motions equal to 3/2 times of the design base earthquake (DBE) ground motions, the measured roof drift capacity is 57% higher than the permissible drift under MCE ground motions. This confirms the sufficient reserve strength and high efficiency of the beam–column joint confined by beams on three faces (Figure 6), despite it lacks shear reinforcement.

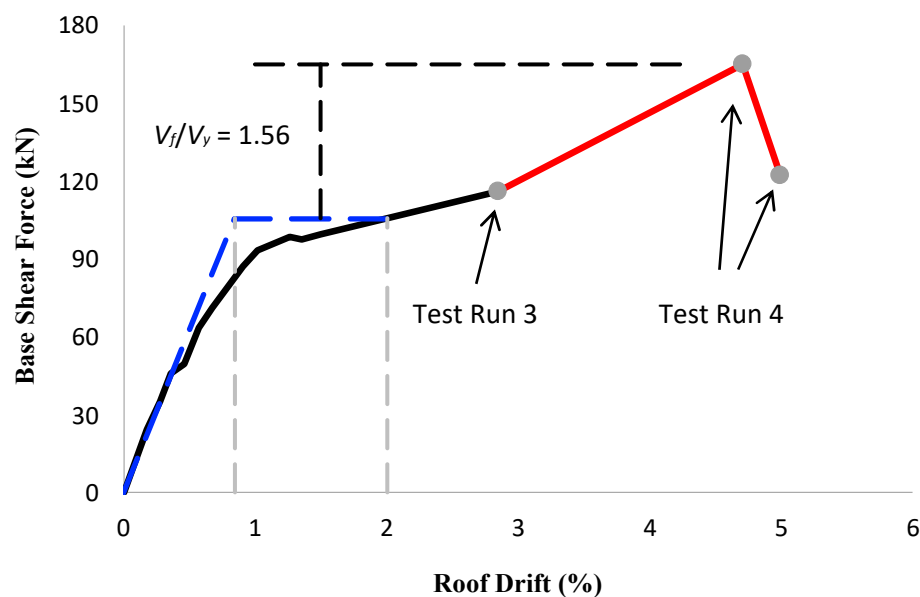


Figure 14. Complete capacity curve for prototype of tested frame till beam–column joints were extensively damaged.

5.2. Shear Strength of Beam–Column Joint

Joint C of the frame was analyzed for determination of joint shear strength. For test run 4, from the forces [108 kN, 54 kN] for roof and first floor, respectively, the corresponding story shear forces $V_S = [54 \text{ kN}, 81 \text{ kN}]$ were obtained for column CE and AC, respectively. This gives bending moments at the joint $M_c = [98 \text{ kN-m}, 147 \text{ kN-m}]$ for column CE (at the base end) and column AC (at the top end), respectively. The point of contraflexure is assumed as the mid-height of the column for computing moments at the column end. The equilibrium of bending moments at the joint will require the bending moment in the beam equal to 246 kN-m. This gives flexural overstrength of beam equal to 1.85 in comparison to nominal bending moment capacity of beam. This increase is attributed to the material overstrength and slab contribution to flexural strength of beam, as suggested earlier by French and Moehle [30], and recently reported [31]. This develops a maximum tension force $T_{pr,max}$ in the joint equal to 658 kN. The corresponding maximum joint shear force $V_{u,joint,max}$ was found equal to 577 kN using Equation (2) and the experimentally obtained story shear and joint tensile force. This gives overstrength equal to 1.58 for joint shear strength in comparison to nominal shear strength determined in accordance with the ACI-318-19 (18.8.4.3). This confirms the efficacy of the considered beam–column joint (Figure 6) of the selected frame despite its lack of shear reinforcement. However, concrete must have a compressive strength equal to or more than 28 MPa for such satisfactory behavior.

6. Discussions

The damages observed in reinforced concrete frames reported following earthquakes [32] highlight the urgent need for seismic performance evaluations of current structures and

infrastructures, as well as the development of some cost-effective upgrade strategies for future designs. To aid in joint shear transfer, current seismic standards require significant amounts of transverse reinforcement to be provided in beam–column joints of reinforced concrete frames. However, the standards do not offer the necessary information to determine the strength and deformation capacity of frames lacking transverse reinforcement in beam–column joints. Because frame constructions in developing countries are almost typically built without special joint reinforcement, there is an urgent need for viable techniques to improve seismic resistance of RC frames, particularly low-rise when the axial load on the column is less.

The use of spandrel beams to confine the beam–column joint and the use of high-strength concrete (compressive strength ≥ 28 MPa) allow for improved construction of the IMRF with weaker beam–column joints. The present ACI strength model, which is dependent on the connection's configuration and the compressive strength of joint core concrete, served as an inspiration for the envisaged improvement strategy. This was validated for a low-rise two-story frame that was designed using the analytical force-based seismic procedure given in the code and conforms to the earthquake-resistant design concept described in the recent standards. The frame's satisfactory seismic performance is verified through a series of dynamic shaking table tests performed on a 1:3 reduced scale frame. The results indicated that the joint shear capacity has a sufficient overstrength, which is ascribed to the geometry of the connection (joint confined on all three faces) and material overstrength.

To assist practicing engineers, simplified analytical methods are employed to determine the force-deformation response of the selected IMRF, which is critically compared to the experimental response. The formulae and procedures are judged to be promising; however, where adjustments to the formulae are required, they are emphasized. Suggestions are presented for analytical approaches to estimating available seismic force-deformation capacity. Based on the results of the experimental program, analytical approaches for analyzing frame resistance are validated, giving better predictions of performance than the ACI model.

Because the design ensured a beam-sway mechanism under the design level input motions, a caution for numerical modeling technique [33] is to consider material/section overstrength for beam/column members, as the beam provided enough hardening to cause significant damage to the joint panel at large deformation demand. The development of severe damage in the joint core confirms hardening in the joint force-deformation behavior, which is critical for joint nonlinear modeling [34].

7. Conclusions

Based on the preliminary design of the selected frame, the following conclusions are drawn:

1. The analysis of the beam indicates overstrength equal to 1.17 for flexural strength and 1.40 for shear strength. The corresponding flexural and shear overstrength obtained for columns are 1.15 and 2.50, respectively;
2. The factored shear force computed in accordance with the ACI-318-19 provisions 18.4.2.3 (a) and 18.4.2.3 (b) gives roughly similar shear force, with the procedure (a) giving relatively high shear force by 7% in comparison to procedure (b);
3. The updated model for the shear strength of concrete included in ACI-318-19 gives a strength 31% less than the previous simple model;
4. The analytical model gives overstrength equal to 1.17 for the shear capacity of the joint for design base action. This confirms the efficacy of the joint laterally supported by beams on three faces despite its lack of shear reinforcement. However, it must be ensured that the concrete has compressive strength equal to or more than 28 MPa.

Based on the observed seismic performance of the selected moment-resisting frame under series of shake-table tests, the following conclusions are drawn:

1. The selected frame exhibited flexural mechanism in beams under base motions with sustained maximum acceleration up to 0.40 g. Only a few slight cracks were developed in beam–column joints under base motions with a sustained maximum acceleration equal to 0.45 g. The joints incurred extensive damage under base motion with sustained maximum acceleration of 0.70 g;
2. The selected frame achieved an overstrength factor equal to 2.50, which is 20% less than the value suggested by the ASCE/SEI-7-22. The ductility factor determined is equal to 2.40, which is 44% higher than the ductility factor inherently available in the response modification coefficient suggested by the ASCE/SEI-7-22 for the selected frame. This gives a response modification coefficient equal to 6.0, which is 20% higher than the value suggested by the ASCE/SEI-7-22;
3. The available analytical model for yield drifts provided an estimate of the ductility factor 33% less than the experimental value. This is due to the fact that such models are based on the response of beam–column connection sub-assemblages lacking slab effects;
4. The virtual work method based on the presumed beam-sway plastic mechanism predicted the peak base shear of the selected frame at roof drift of 2% with sufficient accuracy; it was slightly overestimated by 7%. However, this method underestimated the maximum resistance of the frame at the roof drift of 4.20% by 31%. This is due to the fact that the method ignored the material overstrength and slab contribution to flexural strength. Re-calculating V_{max} using Equation (8) and amplifying the bending moment capacity of the beam by flexural overstrength of 1.85 gives V_{max} equal to 188 kN. This is approximately 14% higher than the experimentally observed maximum resistance of 165 kN;
5. The efficiency of joint that defines the ratio of force causing failure of the joint to the force developed in the frame at the maximum permissible drift is equal to 1.56 (or 156%). This measured efficiency is significantly higher than the values reported previously [28,29]. This increase is attributed to the material overstrength and the fact that the joint was confined by beams on three faces and the concrete strength is 28 MPa;
6. Analysis of beam–column joints based on the experimental response at the roof drift equal to 4.70% gives overstrength equal to 1.58 for joint shear strength in comparison to nominal shear strength determined in accordance with the ACI-318-19 (18.8.4.3). The measured high overstrength confirms the efficacy of the beam–column joint confined by beams on three faces despite the fact it lacks shear reinforcement. However, it is a must to use concrete that has compressive strength equal to or more than 28 MPa. The inherent minimal confinement is sufficient to ensure satisfactory seismic behavior.

Author Contributions: Conceptualization, N.A. and S.H.; methodology, N.A., S.H. and M.R.; software, N.A., S.H. and H.S.; validation, AA. and M.R.; formal analysis, N.A. and S.H.; investigation, N.A. and S.H.; resources, N.A., S.H., H.S., A.A. and M.R.; data curation, N.A. and S.H.; writing—original draft preparation, N.A. and S.H.; writing—review and editing, H.S., A.A. and M.R.; visualization, N.A. and S.H.; supervision, N.A. and M.R.; project administration, N.A. and M.R.; funding acquisition, S.H. All authors have read and agreed to the published version of the manuscript.

Funding: This research received no external funding.

Data Availability Statement: All data sets, models, codes, and programs relevant to the study can be requested from the authors by sending a request to drnaveed@stanford.edu.

Acknowledgments: The authors are grateful to the Board of Advanced Studies and Research (BOASAR) of UET Peshawar for financing the experimental part of the present research work and similar ongoing research projects of postgraduate students.

Conflicts of Interest: The authors declare that they have no known financial conflicts of interest or close personal relationships that may have seemed to have influenced the research described in this study.

Notation

A_j	joint area
A_S	area of longitudinal steel reinforcement in tension
C_d	deflection amplification factor
C_S	seismic response coefficient
C_u	coefficient for upper limit on fundamental time period, 1.5 for SD1 equal to 0.20
C_{vx}	Vertical distribution factor
E	effect of earthquake-induced forces
E_c	Young's modulus of concrete
E_s	Young's modulus of steel
F_x	lateral seismic design forces at level x
$F_{x,f}$	lateral seismic forces at level x at lateral force causing failure of the joint
f'_c	compressive strength of concrete
f_y	yield strength of steel
g	acceleration due to gravity equal to 32.17 ft/s ² (9.81 m/s ²)
h_b	depth of beam
h_{sx}	story height below level x
I_e	earthquake importance factor based on the use and occupancy of the frame
L_b	length of beam
M_{m0}	floor mass of test model
M_{mf}	additional floor mass for test model
M_n	nominal moment strength
M_{nb}	the sum of the nominal flexural strengths of the beams that framing into the joint and measured at the faces of the joint
M_{nc}	the sum of the nominal flexural strengths of the columns that framing into the joint and measured at the faces of the joint
M_{p1}	floor mass of prototype of test model
M_{pb}	plastic moment of beam section
M_{pc}	plastic moment of column section
M_r	prototype-to-model mass ratio
M_u	factored design moment
P_u	factored axial load
R	response modification coefficient
R_μ	ductility factor
S_{DS}	design spectral response acceleration parameter in the short period range
S_{D1}	design spectral response acceleration parameter for structural period equal to 1.0 s
S_L	scale factor
s	center-to-center spacing of transverse reinforcements (ties)
T	fundamental period of the frame
T_{pr}	tensile force in longitudinal reinforcement of beam in tension
V	design lateral strength, design base shear force
V_c	shear strength of concrete
V_{col}	column shear force
V_f	peak lateral force causing failure of the joint
V_{max}	maximum lateral strength, up to permissible maximum design drift
V_n	nominal shear strength
V_S	story shear force
V_u	factored shear force
$V_{n,joint}$	nominal shear strength of joint
$V_{u,joint}$	factored shear strength of joint
W	effective seismic weight of frame
W_{ve}	virtual external work
W_{vi}	virtual internal work
Δ_y	effective yield displacement
Δ_{max}	maximum displacement corresponding to maximum permissible design drift
ε_y	strain of steel corresponding to yield stress
μ	displacement ductility ratio

Ω_o	overstrength factor
ϕ	strength reduction factor
θ	story drift
θ_y	effective yield drift

References

- Gulkan, P.; Sozen, M.A. Inelastic response of reinforced concrete structures to earthquake motions. *ACI Struct. J.* **1974**, *89*, 89–98. [[CrossRef](#)]
- Blume, J.A.; Newmark, N.M.; Corning, L.H. *Design of Multistory Reinforced Concrete Buildings for Earthquake Motions*; Portland Cement Association: Skokie, IL, USA, 1961; 318p.
- Park, R.; Paulay, T. *Reinforced Concrete Structures*; John Wiley & Sons, Inc.: New York, NY, USA, 1975; 768p.
- American Society of Civil Engineers. *Minimum Design Loads and Associated Criteria for Buildings and Other Structures*; ASCE/SEI 7-22; American Society of Civil Engineers: Reston, VA, USA, 2021; 1046p.
- IBC-2021—International Building Code*; International Code Council: Washington, DC, USA, 2020.
- Building Code Requirements for Structural Concrete*; ACI-318-19; American Concrete Institute: Farmington Hills, MI, USA, 2019; 822p.
- Hanson, N.W.; Connor, H.W. Seismic resistance of reinforced concrete beam-column joints. *J. Struct. Div. ASCE* **1967**, *93*, 533–560. [[CrossRef](#)]
- Meinheit, D.F.; Jirsa, J.O. *Shear Strength of Reinforced Concrete Beam-Column Joints*; Report No. 77-1; Department of Civil Engineering, Structures Research Laboratory, University of Texas at Austin: Austin, TX, USA, 1977; 291p.
- Recommendation for Design of Beam-Column Connections in Monolithic Reinforced Concrete Structures—ACI-ASCE Committee 352*; ACI 352R-02; American Concrete Institute: Farmington Hills, MI, USA, 2019; 822p.
- Chopra, K.A. *Dynamics of Structures, Theory and Applications to Earthquake Engineering*, 5th ed.; Prentice Hall: Upper Saddle River, NJ, USA, 2016; 992p.
- Goel, R.K.; Chopra, A.K. Period formulas for moment-resisting frame buildings. *J. Struct. Eng. ASCE* **1997**, *123*, 1454–1461. [[CrossRef](#)]
- Goel, R.K.; Chopra, A.K. Period formulas for concrete shear wall buildings. *J. Struct. Eng. ASCE* **1998**, *124*, 426–433. [[CrossRef](#)]
- Rosenblueth, E.; Contreras, H. Approximate design for multicomponent earthquakes. *J. Eng. Mech. Div. ASCE* **1977**, *103*, 881–893. [[CrossRef](#)]
- Wight, J.K. *Reinforced Concrete: Mechanics and Design*, 7th ed.; Pearson Education Inc.: Hoboken, NJ, USA, 2016; 1144p.
- MacGregor, J.G.; Hanson, J.M. Proposed changes in shear provisions for reinforced and pre-stressed concrete beams. *ACI J. Proc.* **1969**, *66*, 276–288. [[CrossRef](#)]
- Kuchma, D.; Wei, S.; Sanders, D.; Belarbi, A.; Novak, L. Development of the one-way shear design provisions of ACI 318-19. *ACI Struct. J.* **2019**, *116*, 285–295. [[CrossRef](#)]
- Sneed, L.H.; Ramirez, J. Influence of effective depth on the shear strength of concrete beams—Experimental study. *ACI Struct. J.* **2010**, *107*, 554–562. [[CrossRef](#)]
- Bazant, Z.P.; Yu, Q.; Gerstle, W.; Hanson, J.; Ju, J. Justification of ACI 446 code provisions for shear design of reinforced concrete beams. *ACI Struct. J.* **2007**, *104*, 601–610. [[CrossRef](#)]
- Angelakos, D.; Bentz, E.C.; Collins, M.D. Shear strength of large members. *ACI Struct. J.* **2001**, *98*, 290–300.
- Lubell, A.S.; Sherwood, E.G.; Bentz, E.C.; Collins, M.P. Safe shear design of large wide beams. *Concr. Int.* **2004**, *26*, 66–78.
- Brown, M.D.; Bayrak, O.; Jirsa, J.O. Design for shear based on loading conditions. *ACI Struct. J.* **2006**, *103*, 541–550. [[CrossRef](#)]
- Sozen, M.A. Seismic behavior of reinforced concrete buildings. In *Earthquake Engineering*; Bozorgnia, Y., Bertero, V.V., Eds.; CRC Press: New York, NY, USA, 2004; pp. 601–642.
- Moncarz, P.; Krawinkler, H. *Theory and Application of Experimental Model Analysis in Earthquake Engineering*; Report No. 50; Department of Civil and Environmental Engineering, John Blume Earthquake Engineering Center, Stanford University: Stanford, CA, USA, 1981; 263p.
- El-Attar, A.-G.; White, R.N.; Gergely, P. *Shake Table Test of a 1/6 Scale Two-Story Lightly Reinforced Concrete Building*; Report No. 50; Department of Civil and Environmental Engineering, National Center for Earthquake Engineering Research, State University of New York: Buffalo, NY, USA, 1991; 263p.
- Newmark, N.M.; Hall, W.J. *Earthquake Spectra and Design*; Earthquake Engineering Research Institute: Oakland, CA, USA, 1982; 103p.
- Federal Emergency Management Agency (FEMA). *Quantification of Building Seismic Performance Factors*; FEMA-P-695; FEMA: Washington, DC, USA, 2009; 421p.
- Priestley, M.J.N.; Calvi, G.M.; Kowalsky, M.J. *Displacement Based Seismic Design of Structures*; IUSS Press: Pavia, Italy, 2007; 721p.
- Nilsson, I.H.E.; Losberg, A. Reinforced concrete corners and joints subjected to bending moment. *J. Struct. Div. ASCE* **1976**, *102*, 1229–1254. [[CrossRef](#)]
- Balint, P.S.; Taylor, H.P.J. *Reinforcement Detailing of Frame Corner Joints with Particular Reference to Opening Corners*; Technical Report; Cement and Concrete Association: London, UK, 1972; 16p.
- French, C.W.; Moehle, J.P. Effect of floor slab on behavior of slab-beam-column connections. *ACI Symp. Pap.* **1991**, *123*, 225–258. [[CrossRef](#)]

31. Masoudi, M.; Khajevand, S. Revisiting flexural overstrength in RC beam-and-slab floor systems for seismic design and evaluation. *Bull. Earthq. Eng.* **2020**, *18*, 5309–5341. [[CrossRef](#)]
32. Kassem, M.M.; Nazri, F.M.; Farsangi, E.N.; Ozturk, B. Improved vulnerability index methodology to quantify seismic risk and loss assessment in reinforced concrete buildings. *J. Earthq. Eng.* **2022**, *26*, 6172–6207. [[CrossRef](#)]
33. Tariq, H.; Jampole, E.A.; Bandelt, M.J. Development and application of spring hinge models to simulate reinforced ductile concrete structural components under cyclic loading. *ASCE J. Struct. Eng.* **2021**, *147*, 04020322-1–04020322-20. [[CrossRef](#)]
34. Ahmad, N.; Rizwan, M.; Ilyas, B.; Hussain, S.; Khan, M.U.; Shakeel, H.; Ahmad, M.E. Nonlinear Modeling of RC Substandard Beam–Column Joints for Building Response Analysis in Support of Seismic Risk Assessment and Loss Estimation. *Buildings* **2022**, *12*, 1758. [[CrossRef](#)]